the FEBS Journal

Plasmodium falciparum hypoxanthine guanine phosphoribosyltransferase

Stability studies on the product-activated enzyme

Jayalakshmi Raman, Chethan S. Ashok, Sujay I.N. Subbayya, Ranjith P. Anand, Senthamizh T. Selvi and Hemalatha Balaram

Molecular Biology and Genetics Unit, Jawarharlal Nehru Centre for Advanced Scientific Research, Jakkur, Bangalore, India

Keywords
active state stability; hypoxanthine guanine phosphoribosyltransferase; *Plasmodium falciparum*; product activation; thermal stability

Correspondence
H. Balaram, Molecular Biology and Genetics Unit, Jawarharlal Nehru Centre for Advanced Scientific Research, Jakkur, Bangalore 560064, India
Fax: +91 80 22082766
Tel: +91 80 22082812
E-mail: hb@jncasr.ac.in

(Received 20 October 2004, revised 14 February 2005, accepted 18 February 2005)

doi:10.1111/j.1742-4658.2005.04620.x

Hypoxanthine guanine phosphoribosyltransferases (HGPRTs) catalyze the conversion of 6-oxopurine bases to their respective nucleotides, the phosphoribosyl group being derived from phosphoribosyl pyrophosphate. Recombinant *Plasmodium falciparum* HGPRT, on purification, has negligible activity, and previous reports have shown that high activities can be achieved upon incubation of recombinant enzyme with the substrates hypoxanthine and phosphoribosyl pyrophosphate [Keough DT, Ng AL, Winzor DJ, Emmerson BT & de Jersey J (1999) *Mol Biochem Parasitol* **98**, 29–41; Sujay Subbayya IN & Balaram H (2000) *Biochem Biophys Res Commun* **279**, 433–437]. In this report, we show that activation is effected by the product, Inosine monophosphate (IMP), and not by the substrates. Studies carried out on *Plasmodium falciparum* HGPRT and on a temperature-sensitive mutant, L44F, show that the enzymes are destabilized in the presence of the substrates and the product, IMP. These stability studies suggest that the active, product-bound form of the enzyme is less stable than the ligand-free, unactivated enzyme. Equilibrium isothermal-unfolding studies indicate that the active form is destabilized by 2–3 kcal·mol^{-1} compared with the unactivated state. This presents a unique example of an enzyme that attains its active conformation of lower stability by product binding. This property of ligand-mediated activation is not seen with recombinant human HGPRT, which is highly active in the unliganded state. The reversibility between highly active and weakly active states suggests a novel mechanism for the regulation of enzyme activity in *P. falciparum*.

Hypoxanthine guanine phosphoribosyltransferases (HGPRTs) (EC 2.4.2.8) catalyze the conversion of 6-oxopurine bases to their respective mononucleotides, the phosphoribosyl group being derived from phosphoribosyl pyrophosphate (PRPP) in a Mg^{2+}-requiring reaction [1] (Fig. 1A). Most parasitic protozoa do not have the *de novo* purine nucleotide biosynthetic pathway and rely exclusively on the salvage of preformed host purines for their survival [2,3]. Studies by Berman *et al*. show that viability of intraerythrocytic *Plasmodium falciparum* is compromised in the presence of xanthine oxidase and highlight hypoxanthine as the key precursor salvaged for purine nucleotide synthesis [4]. Although weak activities have been reported for adenosine kinase and adenine phosphoribosyltransferase in parasite lysate [5,6], sequences with homology to these enzymes have not been identified in the parasite genome [7]. Purine

Abbreviations
HGPRT, hypoxanthine guanine phosphoribosyltransferase; IMP, inosine monophosphate; PfHGPRT, *Plasmodium falciparum* HGPRT; PRPP, α-D-phosphoribosyl pyrophosphate.

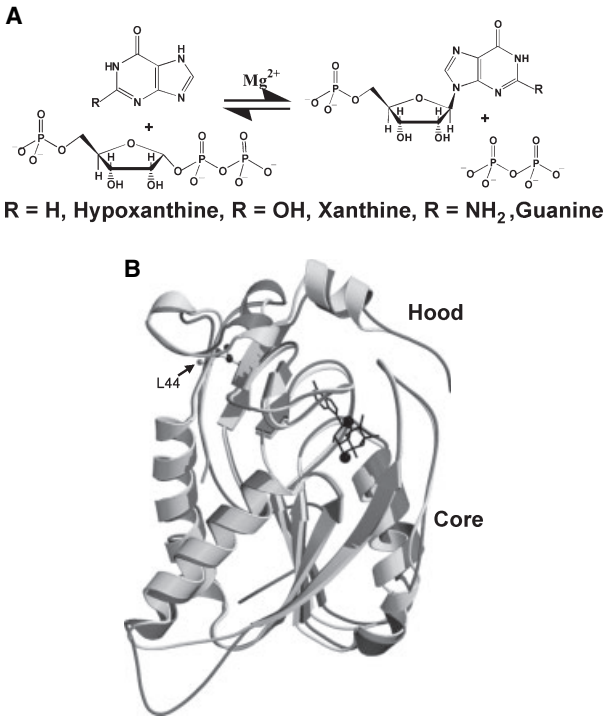

Fig. 1. (A) The reaction catalyzed by HGPRT. (B) Superposition of the transition state analogue, Mg^{2+}, and pyrophosphate bound structures of *P. falciparum* (PDB code 1CJB, black) and human (PDB code 1BZY, grey) HGPRTs. The ligands (from 1CJB), shown in stick representation, define the active site. L44 of PfHGPRT is shown in ball-and-stick representation.

analogs, by serving probably as subversive substrates of HGPRT, have been shown to be lethal to *P. falciparum* in culture [8], making HGPRT a promising drug target. Further evidence for the essentiality of HGPRT to the parasite also comes from the observed antiparasitic activity of antisense oligonucleotides of HGPRT mRNA [9]. However, it should be noted that various other studies have revealed that short oligonucleotides could also exert their action, at high concentrations, as nonspecific polyanions blocking merozite invasion of the erythrocyte [10–13]. HGPRT is also of importance to the host, with the absence and the deficiency of HGPRT manifesting as Lesch–Nyhan syndrome and gouty arthritis, respectively [14,15].

The kinetic mechanism of HGPRT is ordered bi-bi, with PRPP binding first followed by the purine base [16,17]. Product formation has been postulated to occur through a ribo-oxocarbonium ion intermediate [18]. Subsequent to product formation, pyrophosphate release precedes nucleotide release. This mechanism has been elucidated for the human [16], schistosomal [17], *Tritrichomonas foetus* [19] and *Trypanosoma cruzi* [20] HGPRTs, and is also probably true for the *P. falciparum* HGPRT.

Human and *P. falciparum* HGPRTs share a sequence identity of 44% and a similarity of 76%. The structures of both of these enzymes, in complex with transition-state analogues, pyrophosphate and two Mg^{2+} ions, solved to high resolution (2 Å), superpose with an rmsd of $\approx$1.7 Å [21,22] (Fig. 1B). The structure comprises core and hood subdomains, with a cleft between these subdomains forming the active site. The residues contacting the active-site ligands are identical in the two enzymes. Both enzymes are active as homotetramers. Despite this high degree of sequence and structural similarity, these HGPRTs differ significantly in their properties. One difference is in the substrate specificity, the parasite enzyme having the ability to catalyze the phosphoribosylation of xanthine, in addition to hypoxanthine and guanine [23]. Substrate specificity has been shown to be modulated by both active-site and nonactive-site mutations. Mutation of Asp193 to Asn in the active site of *T. foetus* HGPRT results in the loss of activity on xanthine [24]. Mutation of Phe36 (a residue distal from the active site in human HGPRT) to Leu results in an enzyme with activity on xanthine [25]. A chimeric HGPRT, with the N-terminal region in the human enzyme replaced by that of *P. falciparum* HGPRT (PfHGPRT), also has xanthine phosphoribosylation activity [26].

Another difference between these two homologs lies in the behaviour of the purified recombinant enzymes. The recombinant human HGPRT is highly active upon purification, even in the absence of substrates [16]. This is also true of *T. cruzi* HGPRT [27]. In the case of the *Schistosoma mansoni* and *Toxoplasma gondii* HGPRTs, the presence of PRPP stabilizes the enzyme [28,29]. In contrast, the purified *P. falciparum* HGPRT has negligible activity [30,31]. The presence of PRPP alone does not stabilize enzyme activity [30]. The lack of activity has hampered detailed biochemical characterization of the parasite enzyme and raised doubts about the necessity of the enzyme to the parasite [32]. Keough *et al.*, for the first time, showed that the incubation of recombinant PfHGPRT with the substrates hypoxanthine and PRPP, results in a large increase in the specific activities of the enzyme [30]. Oligomerization is also a necessary, but insufficient, condition for activation, with activation being most stable under conditions in which the enzyme is a tetramer. PfHGPRT is a tetramer in low-ionic-strength buffers (10 mM potassium phosphate, pH 7.0). High specific activity can be obtained only upon addition of the substrates to this tetrameric enzyme [30,31]. However, the presence of the substrates does not lead

to activation when the enzyme is a dimer (10 mM potassium phosphate, 1.2 M KCl) [30]. The reported structure of PfHGPRT, in complex with a transition-state analogue inhibitor, immucillin HP, being similar to that of other active HGPRTs represents the active form [22]. Indeed, incubation of unactivated PfHGPRT with the transition state analogue, immucillin GP, followed by removal of the inhibitor by dilution, has been reported to lead to an increase in activity of the enzyme [18].

In this work, we show that the parasite enzyme is activated by the product of the HGPRT reaction, Inosine monophosphate (IMP), and not by the substrates hypoxanthine and PRPP. We also examine the stability of PfHGPRT and a temperature-sensitive mutant, L44F, in the presence and absence of ligands. Temperature and chemical denaturation studies of these enzymes show that the active, product-bound form of PfHGPRT is less stable than the unactivated form.

Results

Our attempts at exploring the structural basis for the xanthine specificity of HGPRTs by random mutagenesis led to the identification of a mutant of the human enzyme, F36L, with xanthine phosphoribosylation activity. A corresponding mutation in the *P. falciparum* enzyme, L44F, led to a decrease in k_{cat} and an increase in the K_m for xanthine [25]. The studies presented here relate to the activity and stability of wild-type PfHGPRT and of the L44F mutant.

In vivo stability of PfHGPRT and L44F

The expression of a functional HGPRT can be monitored by using a complementation assay in *Escherichia coli* Sϕ609 [33,34]. This *E. coli* strain lacks both *de novo* and salvage pathways for purine nucleotide biosynthesis, and growth in minimal medium supplemented with a purine base can be made conditional to the expression of a functional HGPRT [34]. Figure 2A shows the ability of PfHGPRT and the mutant, L44F, to complement the HPRT deficiency in *E. coli* Sϕ609. Examination of the ability of PfHGPRT and L44F to complement the HGPRT deficiency of this strain at 20, 37 and 42 °C showed that the L44F mutant is temperature sensitive. While PfHGPRT permits the growth of these cells at all three temperatures, L44F does so only at 20 and 37 °C. Cells transformed with the L44F expression construct in minimal medium supplemented with the purine base hypoxanthine do not grow at 42 °C (Fig. 2A).

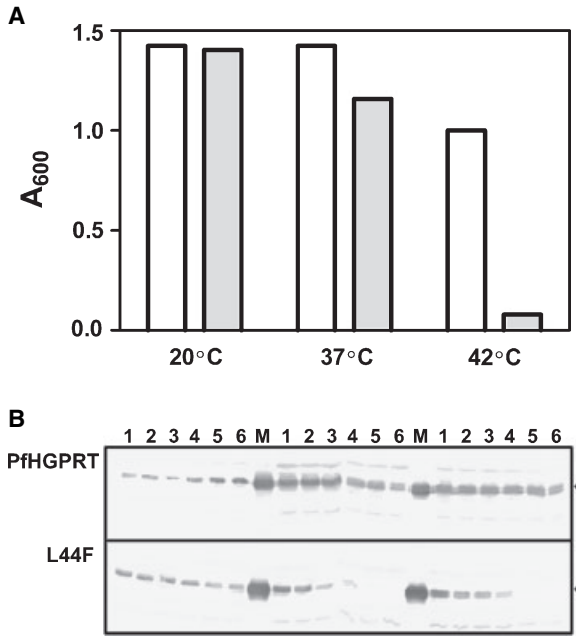

Fig. 2. *In vivo* temperature stability of PfHGPRT and L44F. (A) Growth, at the indicated temperatures, in minimal medium supplemented with hypoxanthine, of *E. coli* Sϕ609 transformed with PfHGRPT (open bars) and L44F (closed bars) expression constructs in pTrc99A. (B) Residual levels of PfHGPRT and L44F, at different incubation temperatures, in Sϕ609 after translational arrest with chloramphenicol. Protein expression was induced by the addition of isopropyl thio-β-D-galactoside and allowed to proceed for 4 h, translation was arrested by the addition of chloramphenicol, and residual protein in aliquots withdrawn at different time-points was detected by western blots probed with polyclonal antibodies against PfHGPRT. Lanes 1–6 represent samples withdrawn at 0, 10, 30, 60, 180 and 300 min, respectively, after the addition of chloramphenicol. M indicates purified PfHGPRT used as a marker. Expression analysis was repeated four times. The temperatures indicated are for both A and B.

Although wild-type PfHGPRT hyper-expresses in Sϕ609, the expression of L44F cannot be detected in Coomassie stained gels, raising the possibility that the failure of L44F to complement could be due to lack of its expression. The expression and stability of both of these proteins were therefore examined by detecting the residual amount of protein after translational arrest with chloramphenicol (Fig. 2B). While the wild-type enzyme was found to be stable at all three temperatures examined, L44F, although expressed, was completely degraded within 1 h of translational arrest at 37 and 42 °C. The mutant protein was, however, found to be stable at 20 °C. The temperature sensitivity of the mutant *in vivo* thus arises as a result of the proteolytic degradation of the protein, probably owing to misfolding at higher temperatures.

Activation of PfHGPRT

Recombinant PfHGPRT is highly soluble and can be readily purified to homogeneity from *E. coli* expression systems [30,31]. Figure 3 compares the far-UV CD spectrum of this purified protein with that of recombinant human HGPRT. Also shown is the CD spectrum of the L44F mutant of PfHGPRT. The spectra show that all three enzymes are largely folded with similar secondary structural composition. Despite this, PfHGPRT and the L44F mutant show negligible activity [25,30,31], while the human enzyme has high activity [16]. Previous reports have shown that considerable improvement in specific activity can be obtained upon incubation of this folded, but largely inactive, enzyme with the substrates hypoxanthine and PRPP in 10 mM potassium phosphate buffer, pH 7.0, conditions under which the enzyme is a tetramer [30,31]. These studies also show that tetramer formation is a necessary, but insufficient, condition for obtaining stable, high activities [30]. L44F, a mutant of the parasite enzyme, also exhibited this property, with high specific activity obtained only upon incubation with the substrates. The activation process is also accompanied by the disappearance of a lag phase that is seen in assays carried out with the unactivated enzyme, suggesting a role for a substrate-induced conformational change in the activation process (data not shown).

Figure 4 shows the specific activity of the wild-type enzyme for xanthine phosphoribosylation after incubation with various combinations of ligands. It should be noted here that specific activities were determined by using a continuous spectrophotometric assay. Initial rates were determined from the difference in absorbance, at different time-points, on the linear phase of the reaction. Any contribution to the absorbance from the ligand carried over (< 0.48 μM) into the assay together with the activated enzyme would not affect the specific activities presented. The presence of ligands at these concentrations in the assay did not increase the reaction rates of the unactivated enzyme. Surprisingly, activation was observed only upon incubation with PRPP and hypoxanthine, and not with guanine and xanthine, the other purine substrates of the enzyme. Although no metal ions were added to the activation mix, the presence of EDTA, in addition to hypoxanthine and PRPP, prevented activation. As the binding of PRPP to HGPRT is dependent on the presence of Mg^{2+} ions [21,22], EDTA could hamper PRPP binding. This suggests that the presence of trace metal ions, probably copurifying with the enzyme, are necessary for the activation process. This also raises the possibility that incubation with the substrates hypoxanthine and PRPP, albeit in the absence of additional Mg^{2+}, might be accompanied by formation of the product, IMP.

Product formation in the activation mix was therefore monitored by the use of ^{3}H-labelled hypoxanthine in

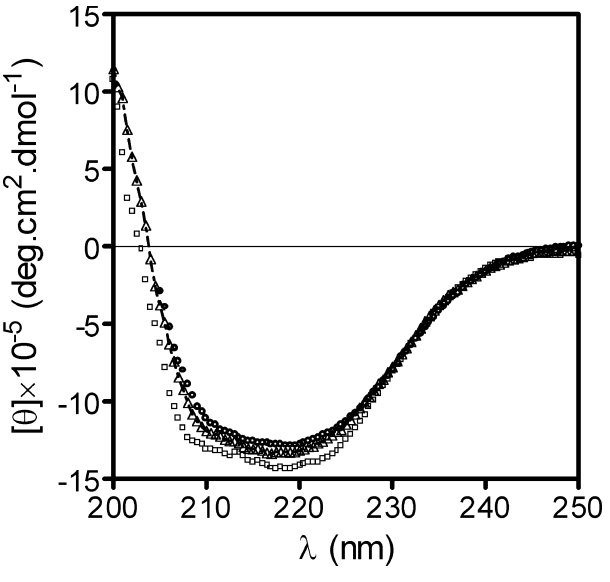

Fig. 3. Far-UV CD spectra of human HGPRT (○),PfHGPRT (△) and L44F (●), in 10 mM potassium phosphate, pH 7.0.

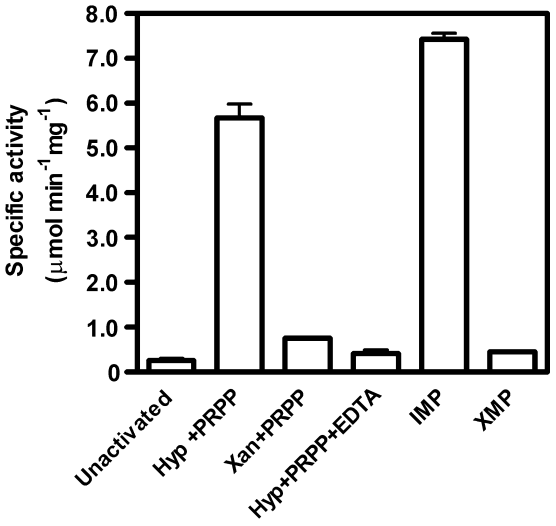

Fig. 4. Specific activity of PfHGPRT after incubation with the indicated ligands. Specific activity for xanthine phosphoribosylation was measured after incubation of PfHGPRT with the ligands for 12 h at 4 °C. Ligand concentrations, when used, were as follows: PRPP, 200 μM; hypoxanthine and IMP, 60 μM; xanthine and XMP, 120 μM; and EDTA, 1 mM, at a protein concentration of 30 μM in 10 mM potassium phosphate, pH 7.0, containing 20% (v/v) glycerol and 5 mM dithiothreitol. Unactivated enzyme refers to the incubation of enzyme in the absence of the ligands under the same buffer conditions.

Table 1. Specific activity of PfHGPRT and concentration of IMP formed at different time-points during activation.

Specific activity ($nmol \cdot min^{-1} \cdot mg^{-1}$)	Time (h)	[IMP] (μM)
1446	6	8
5224	48	38

the activation process. Surprisingly, significant amounts of IMP were detected, although no exogenous metal ions were added to the activation mix. The concentration of IMP formed correlated directly with the degree of activation (Table 1). Indeed, rapid activation could be achieved with IMP. While incubation with hypoxanthine and PRPP took up to 24 h to yield stable activities, IMP could activate the enzyme within 3 h. The final levels of activity obtained in either case were, however, similar. Although substoichiometric IMP concentrations did not lead to complete activation, co-operative activation of the HGPRT homotetramer by IMP binding to one of the subunits cannot be ruled out. Surprisingly, despite the fact that guanosine monophosphate (GMP) and xanthosine monophosphate (XMP) are also products of the PfHGPRT reaction, these nucleotides do not activate the enzyme. The activation process is also completely reversible. The loss of activity, on storage, of some preparations of the enzyme after activation could be traced to the presence of a contaminating phosphatase activity in these preparations. The addition of fresh IMP to these preparations restored the enzyme activity to maximal levels. In the following stability studies, activated enzyme refers to the product (IMP)-bound, highly active form of the enzyme.

Effect of reaction temperature on activity

As the L44F mutant is temperature sensitive, the activity of the mutant at elevated temperatures can be compared to that of the wild-type enzyme. To investigate this, we monitored the phosphoribosylation activity of activated enzyme in reactions initiated by adding the enzyme to preheated assay buffer. Consistent with its temperature sensitivity, the temperature optima for the reactions catalyzed by L44F were lower than that of the wild-type enzyme. Surprisingly, in the case of both enzymes, the temperature optimum for the xanthine reaction was ≈ 10 °C lower than that for the hypoxanthine reaction (Fig. 5A,B). Under similar assay conditions, the xanthine and hypoxanthine phosphoribosylation activities of a xanthine active mutant of human HGPRT, F36L, were found to increase linearly with temperature (Fig. 5C). This differentiation between the substrates hypoxanthine and xanthine is therefore a property of the parasite enzyme. These data gave the first indication that PfHGPRT could be destabilized by its substrates.

Temperature stability, as monitored by CD

The temperature vs. activity profiles of both PfHGPRT and the L44F mutant suggested that the stability of the enzymes in the presence of xanthine and hypoxanthine might be different. This possibility was investigated by monitoring, by CD, the loss of secondary structure in the presence of the substrates as a function of temperature. Initial measurements were carried out with unactivated protein incubated for only 30 min with the substrates. Surprisingly, changes in the stability of the proteins were evident, even at the level of the secondary structure. While the presence of either hypoxanthine or xanthine, along with PRPP, altered the melting behaviour of both enzymes after only 30 min of incubation, the effect was more pronounced in the case of the L44F mutant. The sharp, single transition with a T_m of 64.3 °C, in the melting profile of unliganded (unactivated) L44F, indicative of

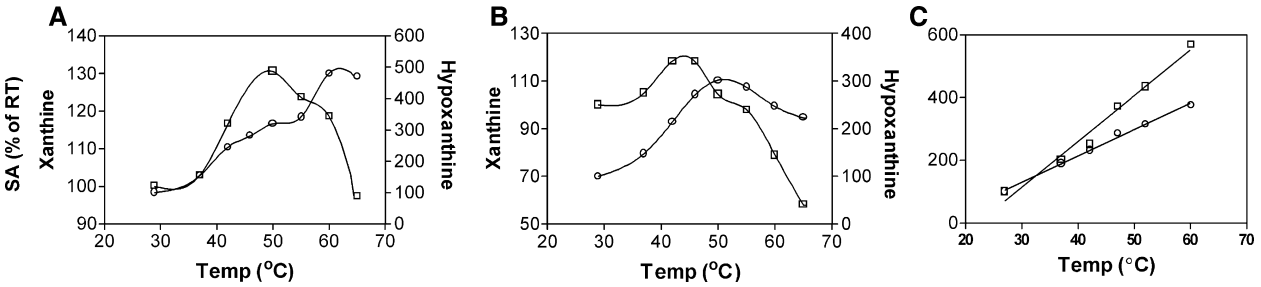

Fig. 5. Specific activity, at different incubation temperatures, expressed as the percentage of activity at room temperature of (A) PfHGPRT, (B) L44F and (C) F36L mutant of human HGPRT on hypoxanthine (○) and xanthine (□). Initial rates were measured by the addition of enzyme to preheated assay buffer by using a spectrophotometer equipped with a water-jacketed cell holder. The curves are representative of two independent experiments with different batches of enzyme.

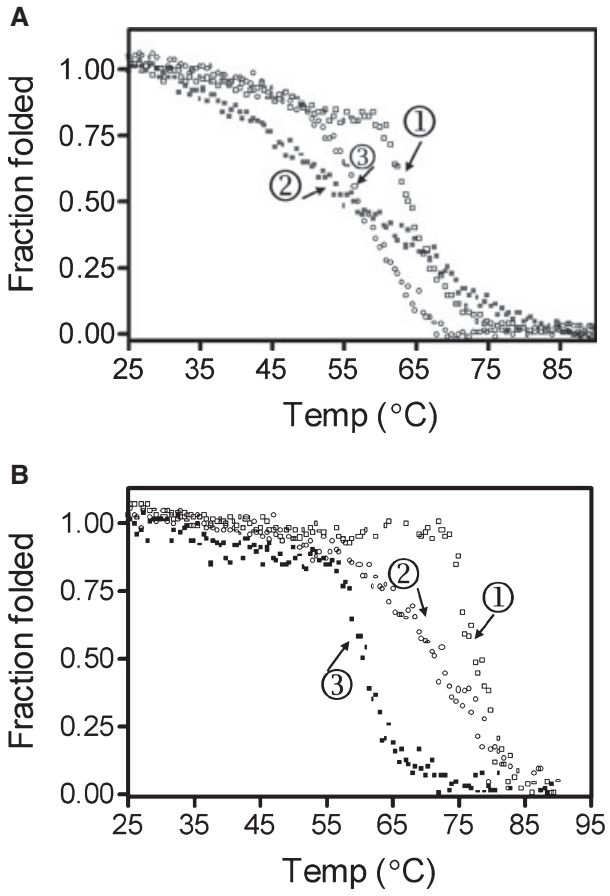

Fig. 6. Temperature denaturation of (A) L44F in the absence of ligands (1) and in the presence of 100 μM α-D-phosphoribosyl pyrophosphate (PRPP) and either 30 μM hypoxanthine (2) or 60 μM xanthine (3). (B) Temperature denaturation of PfHGPRT in the absence of any ligand (1), in the presence of 60 μM IMP (2), or in the presence of 30 μM hypoxanthine and 100 μM PRPP (3). PfHGPRT was preincubated for 15 h at 4 °C in the presence of IMP (2) or hypoxanthine and PRPP (3), before the measurements were made. Denaturation of 2.4 μM protein in 10 mM potassium phosphate buffer, pH 7.0, was monitored by following the CD signal at 220 nm.

co-operativity, altered to a multistate transition in the presence of hypoxanthine and PRPP. In the presence of xanthine and PRPP, the T_m dropped to 57 °C, although the transition profile remained unaltered (Fig. 6A). The melting profiles were not altered in the presence of either PRPP or the purine base alone. These melting profiles suggest that the enzyme is destabilized not only in the presence of xanthine and PRPP, but also on formation of the enzyme/hypoxanthine/PRPP ternary complex, conditions that represent those used for activation of the enzymes.

Pronounced changes in stability of the wild-type enzyme were observed when the stability was monitored after activation of the enzyme. The melting profiles of the wild-type enzyme, after activation, by incubation with either hypoxanthine and PRPP or IMP were compared with those of the unactivated enzyme (Fig. 6B). For these measurements, the enzyme (after overnight activation) was diluted into buffers that represent the initial condition of activation (10 mM potassium phosphate, pH 7.0, containing either 60 μM IMP or 30 μM hypoxanthine and 100 μM PRPP). The melting profile in the presence of hypoxanthine and PRPP thus represents that of an enzyme/PRPP/hypoxanthine ternary complex of the activated enzyme, while the melting profile in the presence of IMP represents that of the activated enzyme bound to IMP. The melting temperature of the activated enzyme, under both of these conditions, is significantly lower than that of the unactivated protein (Fig. 6B). The presence of hypoxanthine and PRPP destabilizes the protein more than the presence of IMP. Together, these melting profiles clearly indicate that the thermal stability of the activated (ligand bound) enzyme is lower than that of the unactivated (unliganded) protein.

Effect of temperature on the equilibrium between high and low activity states

Activated PfHGPRT, in the presence of IMP, was preincubated at different temperatures, and the specific activity of aliquots withdrawn at different time-points was determined at room temperature. The specific activity as a function of preincubation time at different temperatures is shown in Fig. 7A. A sharp decrease in the activity to a value where it is stable for many hours is seen at all temperatures. The value at which the activity stabilizes decreases with increase in preincubation temperature. The value at this plateau, even at 50 °C, is greater than the specific activity of the unactivated enzyme. The drop in activity was found to be completely reversible, with activity returning to initial levels upon lowering the temperature to 4 °C. The existence of stable plateaus suggested an equilibrium process between forms of low and high activity. The K_{eq} at each temperature was determined by using a value corresponding to the activity of the enzyme incubated at 4 °C as the specific activity of the fully activated enzyme, and the value obtained for the enzyme immediately after purification as the specific activity of the unactivated enzyme. The ratio of the concentration of the two species (weakly active 'I' and highly active 'A') can be calculated as:

$$K_{eq} = x/(1 - x),$$

where x is the fraction of A, and

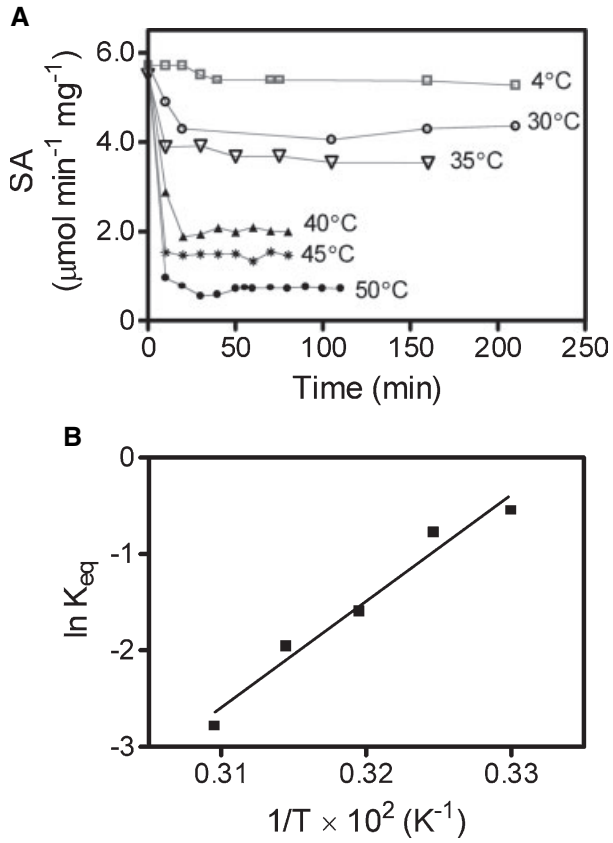

Fig. 7. Effect of temperature on the equilibrium between the high and low activity states of PfHGPRT. (A) Effect of preincubation of activated PfHGPRT at different temperatures on the specific activity for xanthine phosphoribosylation measured at 28 °C. The enzymes were first activated by overnight incubation with 60 μM IMP at 4 °C. Data are representative of three independent experiments. Similar profiles were obtained with L44F. (B) van't-Hoff plot for determination of enthalpy change for the equilibrium I ⇌ A (weakly active ⇌ highly active). The K_{eq} was calculated by using the specific activities recorded at the plateaus at each temperature in (A).

$$x = (SA)_T - (SA)_I/(SA)_A - (SA)_I,$$

for the equilibrium I ⇌ A, where $(SA)_T$ is the specific activity at any temperature T, $(SA)_I$ is the specific activity of the unactivated enzyme, and $(SA)_A$ is the specific activity of the fully activated enzyme.

A van't-Hoff plot (inverse of temperature vs. ln K_{eq}) gives a negative value for ΔH for the I → A transition (Fig. 7B).

Equilibrium isothermal unfolding

The irreversibility of the thermal melting prevents evaluation of the free energies of the activated and unactivated states. Both unactivated and activated PfHGPRT are remarkably stable to denaturation by urea. A significant amount of secondary structure is retained, even at a urea concentration of 8 M. Unfolding studies on the activated and unactivated enzyme were therefore carried out with guanindium chloride. Equilibrium isothermal unfolding with guanidinium chloride at 25 °C placed the free energies of unfolding of the unactivated and activated forms of PfHGPRT at 8.8 ± 0.7 and 6.3 ± 0.2 kcal·mol^{-1}, respectively. By comparison to the unactivated form, the activated form is thus destabilized by 2–3 kcal·mol^{-1} at 25 °C (Fig. 8). As the free energy for this transformation is positive, while the enthalpy change for I → A is negative, the activation of PfHGPRT is entropically unfavorable.

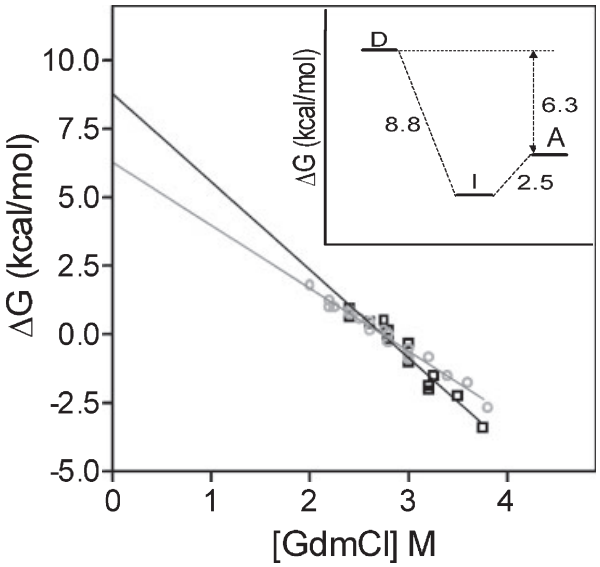

Fig. 8. Free energy for guanidinium chloride (GdmCl) denaturation of unactivated and activated PfHGPRT. Equilibrium unfolding at 25 °C, of activated (○) and unactivated (□) PfHGPRT, at different concentrations of the denaturant, was followed as the CD signal at 220 nm, and the free energy of unfolding was calculated after correction for linear folded and unfolded baselines. The difference between the free energy of the two states is the difference between the value extrapolated to 0 M denaturant. The graph presents data from three independent experiments. Denaturation of the unactivated enzyme was carried out in 10 mM potassium phosphate, pH 7.0, while the activated enzyme was denatured in the presence of 60 μM IMP, both at a protein concentration of 10 μM. The inset shows the proposed energy landscape for the activation process. D, I and A refer to the denatured, weak activity and high activity states of PfHGPRT, respectively. The numbers indicated are free energies derived from equilibrium unfolding studies. See the text for standard error values.

Discussion

The observations described above suggest that the conformation of PfHGPRT on purification is one of high

stability, albeit low activity. Incubation with (and binding of) the substrates/products alters the conformation to a less stable state. This state of lower stability – a metastable state – is the active form of the enzyme. The activity vs. temperature profiles of both PfHGPRT and L44F show that they are destabilized in the presence of xanthine as compared to hypoxanthine, an indication of substrate-induced destabilization. The denaturation profiles of the proteins under activation conditions clearly show that the activated form (IMP bound) is less stable than the unactivated protein. Taken together, these data allow a description of the energy landscape for the activation (Fig. 8, inset), which places the active form 2–3 kcal·mol^{-1} higher than the inactive form.

Metastable active states are infrequently mentioned in the literature. Examples include the class of protease inhibitors, serpins, which lose their inhibitory activity when stabilizing mutations are introduced [35,36]. A well-documented example is the α-lytic protease, the active metastable state of which is achieved with the aid of a pro-segment [37–39]. In PfHGPRT, the product of the reaction, IMP, seems to play a role similar to that of the pro-segment. However, unlike the α-lytic protease that is trapped in the metastable state by a large kinetic barrier [39], PfHGPRT readily reverts to the stable, weakly active form on removal of IMP. The active form, free of IMP, could not be isolated despite repeated attempts. However, the activated enzyme can proceed through repeated cycles of catalysis on all three substrates (hypoxanthine, guanine and xanthine), even after IMP is diluted out in the assay buffer. The process of activation and catalysis is schematically represented in Fig. 9. Although co-operativity has not been observed in HGPRTs, the binding of IMP to one subunit in the inactive tetramer of PfHGPRT, and thus triggering a conformational switch to the active form in the other subunits, could underlie the process of activation. The activated enzyme, capable of binding PRPP and hypoxanthine, is then catalytically competent. Instability of the active form of PfHGPRT indicates that this form is strained and slips back to the inactive state once IMP is removed. This feature of PfHGPRT could stem from its quaternary structure, and differences in interface interactions may be responsible for suppressing co-operativity in other HGPRTs. However, it is interesting to note that co-operativity in PRPP binding has been observed in the human HGPRT mutants, K68A and D194E, with Hill coefficients of 1.9 and 2.3, respectively, while the wild type is nonco-operative [40,41]. A possible structural basis for co-operativity comes from the crystal structures of the trypanosomal and *T. gondii* HGPRTs [42–44]. In the crystal structure of trypanosomal HGPRT, K68 interacts with PRPP and with residues in the neighbouring subunit of the dimer. Elimination of these interactions in the mutant K68A has been suggested to play a role in the observed co-operativity. In the high-resolution structure of the *T. gondii* HGPRT complexed to XMP and pyrophosphate, a network of hydrogen bonds, direct and water-mediated, linking the active site in one subunit with that in the adjacent subunit of the tetramer, also provides a structural basis for the co-operativity seen in the mutants. The only available structure of PfHGPRT is of a complex with a transition state analog representing the active state. Structures of unliganded and different substrate/product complexes should

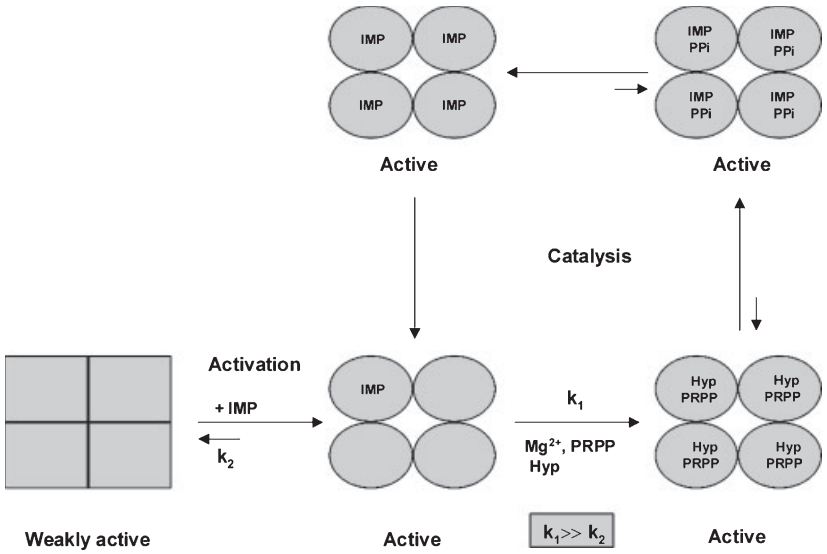

Fig. 9. Schematic representation of the process of activation and catalysis by PfHGPRT. IMP binding switches the enzyme from a weak to a high activity state, and its removal reverts the enzyme back to weak activity. Our model shows that IMP binding to one subunit may be sufficient to retain the high activity state of the tetramer, with active sites in the remaining subunits available for catalysis. The enzyme remains active during the assay owing to the faster rate of α-D-phosphoribosyl pyrophosphate (PRPP)/hypoxanthine binding (k_1) compared to the rate of conversion to the weakly active state on IMP release (k_2). Hyp, hypoxanthine; PPi, pyrophosphate. 'Active' refers to the high activity state of PfHGPRT.

provide insights into the mechanism of activation of PfHGPRT.

Native state metastability has been proposed to have varied biological significance. In the α-lytic protease, it represents a mechanism for increasing protease longevity [37,38]. The decreased conformational flexibility of the native metastable state of the mature protease protects it from proteolytic degradation [39]. In the case of the protease inhibitors, serpins, metastability has been suggested to be a mechanism for regulation, presumably facilitating a conformational switch allowing inhibition [36]. A similar role has also been suggested for hemagglutinin [45] and some viral capsid proteins [46,47], where the metastability permits the conformational switch to a fusion active state. In the phosphoribulokinase/glyceraldehyde-3-phosphate dehydrogenase complex, phosphoribulokinase is in a metastable state immediately after dissociation from the complex and relaxes to a stable state of lower activity, with time, after dissociation [48].

The property of ligand-induced conformational changes to an active state of lower stability is unique to PfHGPRT and is not seen with the human homolog. It provides a mechanism for fast interconversion between a form of low activity and one of high activity, thus providing a means for regulating enzyme activity *in vivo*. However, the precise role of such a regulatory process is not obvious and requires investigation. It is also possible that PfHGPRT may be associated with other cellular proteins *in vivo*, allowing substrate channeling with the association maintaining the protein in the active conformation. The absence of the *de novo* pathway in the malaria parasite entails a central role for HGPRT in the parasites' purine metabolism. The requirements of regulation and activity that this unique position would impose, especially in context of the high A/T content (> 70% AT) of the *P. falciparum* genome [49], may necessitate novel modes for control of enzyme activity. Complete biochemical characterization of all the enzymes of the purine salvage pathway in *P. falciparum* should provide insight into the role of IMP in regulating purine metabolism in the parasite.

Experimental procedures

Restriction enzymes, *Taq* DNA polymerase, T_4 DNA ligase and other molecular biology reagents were purchased from Bangalore Genei Pvt. Ltd (Bangalore, India) or from MBI Fermentas (V. Graiciuno, Vilnius, Lithuania) and used according to the manufacturers' instructions. The *E. coli* strain Sϕ609 (*ara, Δpro-gpt- lac, thi, hpt, pup, purH,J, strA*) was a gift from Dr Per Nygaard, University of Copenhagen (Copenhagen, Denmark). All chemicals used in the assays were from Sigma Chemical Company (St. Louis, MO, USA) and media components were from HiMedia Laboratories Ltd (Mumbai, India). Purine base stocks were made in 0.4 M NaOH, and all other solutions were made in water.

Functional complementation

Complementation studies were carried out by using the *E. coli* strain Sϕ609 (*ara, Δpro-gpt-lac, thi, hpt, pup, purH,J, strA*) [33] transformed with the expression constructs of human HGPRT, PfHGPRT or L44F in pTrc99A. Conditions used for complementation analysis were as described previously [34]. Briefly, cells grown overnight in LB (Luria–Bertani) medium containing ampicillin (concentration 100 μg ml^{-1}) and streptomycin (concentration 25 μg ml^{-1}), were washed with, and resuspended in, 1× M9 salt solution. A 1% (v/v) inoculum of these cells was added to minimal medium containing 1× M9 salts, 1 mM $MgSO_4$, 0.1 mM $CaCl_2$, 1 mM thiamine hydrochloride, 1 mM proline, 0.2% (w/v) glucose, 0.3 mM isopropyl thio-β-D-galactoside, 25 μg·mL^{-1} streptomycin, 100 μg·mL^{-1} ampicillin and 0.5 mM hypoxanthine, guanine or xanthine. The cells were cultured for 15 h at 37 °C and the attenuance (*D*) at 600 nm was recorded. All experiments were repeated at least three times.

Determination of *in vivo* stability

For determination of the *in vivo* stability of PfHGPRT and L44F, Sϕ609 cells containing the expression constructs of these proteins in pTrc99A were grown to reach a D_{600} of 0.6 at 20, 37 or 42 °C, and protein expression was induced by the addition of IPTG to a concentration of 1 mM. Protein translation was arrested by the addition of chloramphenicol to a concentration of 300 μg·mL^{-1} after 4 h of induction. The residual concentration of expressed proteins, in aliquots withdrawn at different time-points, was determined by Western blots probed with antibodies to *P. falciparum* HGPRT.

Protein expression and purification

PfHGPRT was hyper-expressed in *E. coli* Sϕ609 transformed with the expression construct in the vector pTrc99A and purified as described previously [31]. Soluble protein was precipitated with ammonium sulfate and then subjected to anion exchange chromatography using a Q-Sepharose column connected to an AKTA-Basic (Amersham Pharmacia Biotech, Little Chalfont, Buckinghamshire, UK) HPLC system, at pH 8.9. The protein eluting at ≈200 mM NaCl was then subjected to cation exchange chromatography (at pH 6.9) using a Resource S column. The bound protein was eluted with a linear NaCl gradient.

The L44F mutant was cloned into the vector pET23d and expressed in *E. coli* BL21(DE3) [F^- *ompT hsdS*$_B$(r_B^- m_B)

gal dcm (DE3)]. Soluble L44F from lysates obtained after ammonium sulfate fractionation was purified by chromatography on a Cibacron Blue column followed by anion exchange chromatography, with both columns being eluted with increasing gradients of KCl in the presence of 20% (v/v) glycerol in all steps [25]. Finally, both wild-type and L44F enzymes were buffer exchanged, by gel filtration, into 10 mM potassium phosphate, pH 7.0, 20% (v/v) glycerol and 2 mM dithiothreitol, and were found to be greater than 90% pure, as judged by SDS/PAGE.

Protein concentrations were determined by using the method of Bradford, with BSA as a standard [50].

Enzyme activation

PfHGPRT and L44F were activated by incubation with 60 μM hypoxanthine and 200 μM PRPP, or with 60 μM IMP, at a protein concentration of 30 μM in 10 mM potassium phosphate, pH 7.0, 20% (v/v) glycerol, 5 mM dithiothreitol at 4 °C. Stable maximal activities were achieved after ≈24 h with the hypoxanthine/PRPP activations and within 3 h for the IMP activations. For the guanidinium chloride denaturation studies, PfHGPRT was activated at a concentration of 50 μM with IMP at 120 μM.

Detection of product formation during activation

For detection of product formation during activation, activation was carried out with 200 μM PRPP and 60 μM ^{3}H-labelled hypoxanthine (specific activity of 3.1 Ci·mol^{-1}) at a protein concentration of 30 μM in 10 mM potassium phosphate, pH 7.0, 20% (v/v) glycerol, containing 5 mM dithiothreitol. The amount of IMP in activations set up with ^{3}H-labelled hypoxanthine was determined after the separation of hypoxanthine and IMP, in aliquots of the activation mix, by paper chromatography with 2% (v/v) sodium dihydrogen ortho-phosphate as the mobile phase. Spots corresponding to hypoxanthine and IMP were cut out and the radioactivity corresponding to each was determined by liquid scintillation.

Enzyme assays

Activation was routinely monitored by measuring, spectrophotometrically, the specific activity for xanthine phosphoribosylation [51]. Assays were carried out in 100 mM Tris/HCl, pH 7.5, 12 mM $MgCl_2$, containing 200 μM xanthine and 1 mM PRPP. Reactions were initiated by the addition of 2–3 μg of enzyme to 250 μL of the reaction mix, and XMP formation was monitored as an increase in absorption at 255 nm. A Δε value of 3794 M^{-1}·cm^{-1} was used to calculate specific activity. Hypoxanthine and guanine phosphoribosylation reactions were carried out with a purine base concentration of 100 μM, and product formation was monitored at 245 and 257.5 nm, respectively. The Δε values used were 1900 M^{-1}·cm^{-1} and 5600 M^{-1}·cm^{-1} for IMP and GMP formation, respectively [16,30]. Activities at higher temperatures were determined by initiation of the reaction by addition of activated enzyme to assay buffer containing the appropriate substrates preheated to the desired temperature. All reactions were monitored continuously and specific activities are derived from the difference in absorbance between two time-points within which the reaction is linear. Activity was measured by using a Hitachi U2010 spectrophotometer equipped with a water-jacketed cell holder.

CD measurements

CD measurements were carried out in 10 mM potassium phosphate, pH 7.0, on a JASCO-715 spectropolarimeter equipped with a Peltier heating system. The temperature denaturation was measured at a protein concentration of 2.5 μM with a path length of 10 mm and a heating rate of 1 °C·min^{-1}. The guanidinium chloride denaturation measurements were carried out at a protein concentration of 10 μM with a path length of 1 mm. Protein unfolding was monitored as the CD signal at 220 nm. The fraction unfolded (f_U) at each point was determined as:

$$f_U = (\theta_F - \theta)/(\theta_F - \theta_U),$$

where θ_F and θ_U are the ellipticities of the folded and unfolded states at each denaturant concentration after correction for linear baselines, and θ is the measured ellipticity at each denaturant concentration.

The equilibrium constant, *K*, was calculated from the following equation:

$$K = f_U/(1 - f_U)$$

The free energy change (Δ*G*) was calculated from the following equation:

$$\Delta G = -RT \ln K$$

where R is the gas constant (8.3 J·K^{-1}·mol^{-1}) and T the absolute temperature. The free energy change in the absence of denaturant (Δ*G* H_2O) was determined by fitting to:

$$\Delta G = (\Delta G\, H_2O) - m(\text{denaturant concentration})$$

The free energy change for the unfolding of unactivated and activated PfHGPRT was determined in the absence and presence, respectively, of IMP. The difference between these values represents the difference between the stability of these states.

Acknowledgements

This study was supported, in part, by grants from the Department of Biotechnology, Government of India. C.S.A. thanks the Department of Biotechnology for the postdoctoral fellowship. We thank Prof. P. Nygaard,

University of Copenhagen, for the gift of *Eshcerichia coli* Sϕ609. We also thank the Molecular Biophysics Unit, Indian Institute of Science, for allowing us to use the spectropolarimeter.

References

1 Salerno C & Giacomello A (1981) Human hypoxanthine guanine phosphoribosyltransferase. The role of magnesium ion in a phosphoribosylpyrophosphate-utilizing enzyme. *J Biol Chem* **256**, 3671–3673.
2 Ullman B & Carter D (1995) Hypoxanthine-guanine phosphoribosyltransferase as a therapeutic target in protozoal infections. *Infect Agents Dis* **4**, 29–40.
3 Sherman IW (1979) Biochemistry of Plasmodium (malarial parasites). *Microbiol Rev* **43**, 453–495.
4 Berman PA, Human L & Freese JA (1991) Xanthine oxidase inhibits growth of *Plasmodium falciparum* in human erythrocytes *in vitro*. *J Clin Invest* **88**, 1848–1855.
5 Reyes P, Rathod PK, Sanchez DJ, Mrema JE, Rieckmann KH & Heidrich HG (1982) Enzymes of purine and pyrimidine metabolism from the human malaria parasite, *Plasmodium falciparum*. *Mol Biochem Parasitol* **5**, 275–290.
6 Queen SA, Vander Jagt DL & Reyes P (1989) Characterization of adenine phosphoribosyltransferase from the human malaria parasite, *Plasmodium falciparum*. *Biochim Biophys Acta* **996**, 160–165.
7 Gardner MJ, Hall N, Fung E, White O, Berriman M, Hyman RW, Carlton JM, Pain A, Nelson KE, Bowman S *et al*. (2002) Genome sequence of the human malaria parasite *Plasmodium falciparum*. *Nature* **419**, 498–511.
8 Queen SA, Jagt DL & Reyes P (1990) *In vitro* susceptibilities of *Plasmodium falciparum* to compounds which inhibit nucleotide metabolism. *Antimicrob Agents Chemother* **34**, 1393–1398.
9 Dawson PA, Cochran DA, Emmerson BT & Gordon RB (1993) Inhibition of *Plasmodium falciparum* hypoxanthine-guanine phosphoribosyltransferase mRNA by antisense oligodeoxynucleotide sequence. *Mol Biochem Parasitol* **60**, 153–156.
10 Kanagaratnam R, Misiura K, Rebowski G & Ramasamy R (1998) Malaria merozoite surface protein antisense oligodeoxynucleotides lack antisense activity but function as polyanions to inhibit red cell invasion. *Int J Biochem Cell Biol* **30**, 979–985.
11 Ramasamy R, Kanagaratnam R, Misiura K, Rebowski G, Amerakoon R & Stec WJ (1996) Anti-sense oligodeoxynucleoside phosphorothioates nonspecifically inhibit invasion of red blood cells by malaria parasites. *Biochem Biophys Res Commun* **218**, 930–933.
12 Clark DL, Chrisey LA, Campbell JR & Davidson EA (1994) Non-sequence-specific antimalarial activity of oligodeoxynucleotides. *Mol Biochem Parasitol* **63**, 129–134.
13 Barker RH Jr, Metelev V, Rapaport E & Zamecnik P (1996) Inhibition of *Plasmodium falciparum* malaria using antisense oligodeoxynucleotides. *Proc Natl Acad Sci USA* **93**, 514–518.
14 Lesch M & Nyhan WL (1964) A familial disorder of uric acid metabolism and central nervous system function. *Am J Med* **36**, 561–570.
15 Jinnah HA, De Gregorio L, Harris JC, Nyhan WL & O'Neill JP (2000) The spectrum of inherited mutations causing HPRT deficiency: 75 new cases and a review of 196 previously reported cases. *Mutat Res* **463**, 309–326.
16 Xu Y & Grubmeyer C (1998) Catalysis in human hypoxanthine-guanine phosphoribosyltransferase: Asp 137 acts as a general acid/base. *Biochemistry* **37**, 4114–4124.
17 Yuan L, Craig SP, McKerrow JH & Wang CC (1992) Steady-state kinetics of the schistosomal hypoxanthine-guanine phosphoribosyltransferase. *Biochemistry* **31**, 806–810.
18 Li CM, Tyler PC, Furneaux RH, Kicska G, Xu Y, Grubmeyer C, Girvin ME & Schramm VL (1999) Transition-state analogs as inhibitors of human and malarial hypoxanthine-guanine phosphoribosyltransferases. *Nat Struct Biol* **6**, 582–587.
19 Munagala NR, Chin MS & Wang CC (1998) Steady-state kinetics of the hypoxanthine-guanine-xanthine phosphoribosyltransferase from *Tritrichomonas foetus*: the role of threonine-47. *Biochemistry* **37**, 4045–4051.
20 Wenck MA, Medrano FJ, Eakin AE & Craig SP (2004) Steady-state kinetics of the hypoxanthine guanine phosphoribosyltransferase from *Trypanosoma cruzi*. *Biochim Biophys Acta* **1700**, 11–18.
21 Shi W, Li CM, Tyler PC, Furneaux RH, Grubmeyer C, Schramm VL & Almo SC (1999) The 2.0 Å structure of human hypoxanthine-guanine phosphoribosyltransferase in complex with a transition-state analog inhibitor. *Nat Struct Biol* **6**, 588–593.
22 Shi W, Li CM, Tyler PC, Furneaux RH, Cahill SM, Girvin ME, Grubmeyer C, Schramm VL & Almo SC (1999) The 2.0 Å structure of malarial purine phosphoribosyltransferase in complex with a transition-state analogue inhibitor. *Biochemistry* **38**, 9872–9880.
23 Queen SA, Vander Jagt D & Reyes P (1988) Properties and substrate specificity of a purine phosphoribosyltransferase from the human malaria parasite, *Plasmodium falciparum*. *Mol Biochem Parasitol* **30**, 123–133.
24 Munagala NR & Wang CC (1998) Altering the purine specificity of hypoxanthine-guanine-xanthine phosphoribosyltransferase from *Tritrichomonas foetus* by structure-based point mutations in the enzyme protein. *Biochemistry* **37**, 16612–16619.
25 Raman J, Sumathy K, Anand RP & Balaram H (2004) A non-active site mutation in human hypoxanthine guanine phosphoribosyltransferase expands substrate specificity. *Arch Biochem Biophys* **427**, 116–122.

26 Sujay Subbayya IN, Sukumaran S, Shivashankar K & Balaram H (2000) Unusual substrate specificity of a chimeric hypoxanthine-guanine phosphoribosyltransferase containing segments from the *Plasmodium falciparum* and human enzymes. *Biochem Biophys Res Commun* **272**, 596–602.
27 Eakin AE, Guerra A, Focia PJ, Torres-Martinez J & Craig SP (1997) Hypoxanthine phosphoribosyltransferase from *Trypanosoma cruzi* as a target for structure-based inhibitor design: crystallization and inhibition studies with purine analogs. *Antimicrob Agents Chemother* **41**, 1686–1692.
28 Yuan L, Craig SP, McKerrow JH & Wang CC (1990) The hypoxanthine-guanine phosphoribosyltransferase of *Schistosoma mansoni*. Further characterization and gene expression in *Escherichia coli*. *J Biol Chem* **265**, 13528–13532.
29 Heroux A, White EL, Ross LJ & Borhani DW (1999) Crystal structures of the *Toxoplasma gondii* hypoxanthine-guanine phosphoribosyltransferase-GMP and -IMP complexes: comparison of purine binding interactions with the XMP complex. *Biochemistry* **38**, 14485–14494.
30 Keough DT, Ng AL, Winzor DJ, Emmerson BT & de Jersey J (1999) Purification and characterization of *Plasmodium falciparum* hypoxanthine-guanine-xanthine phosphoribosyltransferase and comparison with the human enzyme. *Mol Biochem Parasitol* **98**, 29–41.
31 Sujay Subbayya IN & Balaram H (2000) Evidence for multiple active states of *Plasmodium falciparum* hypoxanthine-guanine-xanthine phosphoribosyltransferase. *Biochem Biophys Res Commun* **279**, 433–437.
32 Olliaro PL & Yuthavong Y (1999) An overview of chemotherapeutic targets for antimalarial drug discovery. *Pharmacol Ther* **81**, 91–110.
33 Jochimsen B, Nygaard P & Vestergaard T (1975) Location on the chromosome of *Escherichia coli* of genes governing purine metabolism. Adenosine deaminase (add), guanosine kinase (gsk) and hypoxanthine phosphoribosyltransferase (hpt). *Mol Gen Genet* **143**, 85–91.
34 Shivashankar K, Subbayya IN & Balaram H (2001) Development of a bacterial screen for novel hypoxanthine-guanine phosphoribosyltransferase substrates. *J Mol Microbiol Biotechnol* **3**, 557–562.
35 Lee C, Park SH, Lee MY & Yu MH (2002) Regulation of protein function by native metastability. *Proc Natl Acad Sci USA* **97**, 7727–7731.
36 Wang Z, Mottonen J & Goldsmith EJ (1996) Kinetically controlled folding of the serpin plasminogen activator inhibitor 1. *Biochemistry* **35**, 16443–16448.
37 Cunningham EL, Jaswal SS, Sohl JL & Agard DA (1999) Kinetic stability as a mechanism for protease longevity. *Proc Natl Acad Sci USA* **96**, 11008–11014.
38 Jaswal SS, Sohl JL, Davis JH & Agard DA (2002) Energetic landscape of alpha-lytic protease optimizes longevity through kinetic stability. *Nature* **415**, 343–346.
39 Sohl JL, Jaswal SS & Agard DA (1998) Unfolded conformations of alpha-lytic protease are more stable than its native state. *Nature* **395**, 817–819.
40 Lightfoot T, Lewkonia RM & Snyder FF (1994) Sequence, expression and characterization of HPRTMoose Jaw: a point mutation resulting in cooperativity and decreased substrate affinities. *Hum Mol Genet* **3**, 1377–1381.
41 Balendiran GK, Molina JA, Xu Y, Torres-Martinez J, Stevens R, Focia PJ, Eakin AE, Sacchettini JC & Craig SP III (1999) Ternary complex structure of human HGPRTase, PRPP, Mg^{2+} and the inhibitor HPP reveals the involvement of the flexible loop in substrate binding. *Protein Sci* **8**, 1023–1031.
42 Focia PJ, Craig SP III & Eakin AE (1998) Approaching the transition state in the crystal structure of a phosphoribosyltransferase. *Biochemistry* **37**, 17120–17127.
43 Focia PJ, Craig SP III, Nieves-Alicea R, Fletterick RJ & Eakin AE (1998) A 1.4 Å crystal structure for the hypoxanthine phosphoribosyltransferase of *Trypanosoma cruzi*. *Biochemistry* **37**, 15066–15075.
44 Heroux A, White EL, Ross LJ, Davis RL & Borhani DW (1999) Crystal structure of the *Toxoplasma gondii* hypoxanthine-guanine phosphoribosyltransferase with XMP, pyrophosphate and two Mg^{2+} ions bound: insights into the catalytic mechanism. *Biochemistry* **38**, 14495–14506.
45 Carr CM, Chaudhry C & Kim PS (1997) Influenza hemagglutinin is spring-loaded by a metastable native conformation. *Proc Natl Acad Sci USA* **94**, 14306–14313.
46 Smith JG, Mothes W, Blacklow SC & Cunningham JM (2004) The mature avian leukosis virus subgroup A envelope glycoprotein is metastable, and refolding induced by the synergistic effects of receptor binding and low pH is coupled to infection. *J Virol* **78**, 1403–1410.
47 Stiasny K, Allison SL, Mandl CW & Heinz FX (2001) Role of metastability and acidic pH in membrane fusion by tick-borne encephalitis virus. *J Virol* **75**, 7392–7398.
48 Lebreton S & Gontero B (1999) Memory and imprinting in multienzyme complexes. Evidence for information transfer from glyceraldehyde-3-phosphate dehydrogenase to phosphoribulokinase under reduced state in *Chlamydomonas reinhardtii*. *J Biol Chem* **274**, 20879–20884.
49 Pollack Y, Katzen AL, Spira DT & Golenser J (1982) The genome of *Plasmodium falciparum*. I: DNA base composition. *Nucleic Acids Res* **10**, 539–546.
50 Bradford MM (1976) A rapid and sensitive method for the quantitation of microgram quantities of protein utilizing the principle of protein–dye binding. *Anal Biochem* **72**, 248–254.
51 Giacomello A & Salerno C (1977) A continuous spectrophotometric assay for hypoxanthine-guanine phosphoribosyltransferase. *Anal Biochem* **79**, 263–267.